A Ground-based Sensor to Detect GEOs Without the Use of a Laser Guide-star

Mala Mateen
Air Force Research Laboratory, Kirtland AFB, NM, 87117
Olivier Guyon
Subaru Telescope, Hilo, HI, 96720
Michael Hart,
Steward Observatory, Tucson, AZ, 85721
Robert Johnson
Air Force Research Laboratory, Kirtland AFB, NM, 87117
Earl Spillar,
Air Force Research Laboratory, Kirtland AFB, NM, 87117

Abstract: We are developing a highly sensitive non-linear Curvature Wavefront Sensor (nlCWFS) which will make it possible to detect objects as dim as $m_v = 11 - 14$. Current Space Situational Awareness (SSA) programs rely on laser guide stars (LGSs) to detect dim objects near GEOs, however LGSs are expensive to use and require permission to lase. The nlCWFS will be able to detect objects near GEOs without the use of a LGS and will be able to obtain higher contrast then possible with the SHWFS.

The nlCWFS senses at the diffraction limit whereas currently used WFSs such as the SHWFS sense at the seeing limit. This difference awards the nlCWFS a gain in photon flux of $(\frac{D}{r_0})^2$ at low spatial modes such as tip-tilt. The SHWFS allows interference of points separated only by a subaperture making it insensitive to low order modes. The nlCWFS, on the other hand, uses the full spatial coherence of the pupil making it sensitive to low order modes which dominate the atmosphere and scatter light within a close angular separation of a GEO where a dim object might be hiding. In order to find dim objects near a bright target it is important to obtain a high contrast ratio within a small angular resolution of the central PSF core. The PSF contrast obtained with the nlCWFS is two orders of magnitude better than the SHWFS.

In this paper we present results from building the nlCWFS for the 6.5 m MMT Smithsonian Observatory. We outline our progress towards building a nlCWFS for a 1.5 m telescope.

1. INTRODUCTION

The non-linear Curvature Wavefront Sensor (nlCWFS) is derived from the successful curvature wavefront sensing principle [1] where the wavefront is measured as a contrast between images acquired on either side of the pupil plane. A linear relationship exists between the two quantities [2]. The linear relationship breaks down at large distances from the pupil plane, this affect is shown in figure 1 where the rays are seen to become non-linear as the distance from the pupil increases. Large propagation distances correspond to high sensitivity to low order modes, as a result, the conventional curvature wavefront sensor (cCWFS) is less sensitive to low order aberrations. The nlCWFS solves this problem by recording the wavefront at several Fresnel planes on either side of the pupil allowing sensitivity to low and high order aberrations. The nlCWFS principle relies on Fresnel propagation to convert pupil plane phase into amplitude modulations, [3],[4],[5] the efficiency with which this phase to amplitude conversion is performed is a function of both the spatial frequency of the phase aberration and the propagation distance. Each Fresnel propagation corresponds to a different spatial frequency and the combination of the spatial frequencies allows the reconstruction of the wavefront in the pupil plane. Figure 2 shows lab data obtained with the nlCWFS. Each frame encodes phase aberrations most efficiently for a specific spatial frequency [6]. It has been determined through numerical simulations that the use of four Fresnel planes is ideal for nlCWFS wavefront reconstruction. Intensity is recorded in four Fresnel planes, two on either side of the pupil. In order to reconstruct the wavefront in the pupil plane the recorded intensities are propagated back and forth, in an iterative Gerchberg-Saxton loop [7], between the pupil plane and the Fresnel

Report Documentation Page

Form Approved
OMB No. 0704-0188

1. REPORT DATE	2. REPORT TYPE	3. DATES COVERED
SEP 2013		**00-00-2013 to 00-00-2013**

4. TITLE AND SUBTITLE	5a. CONTRACT NUMBER
A Ground-based Sensor to Detect GEOs Without the Use of a Laser Guide-star	5b. GRANT NUMBER
	5c. PROGRAM ELEMENT NUMBER
6. AUTHOR(S)	5d. PROJECT NUMBER
	5e. TASK NUMBER
	5f. WORK UNIT NUMBER
7. PERFORMING ORGANIZATION NAME(S) AND ADDRESS(ES) **Air Force Research Laboratory (AFRL),Kirtland AFB,NM,87117**	8. PERFORMING ORGANIZATION REPORT NUMBER
9. SPONSORING/MONITORING AGENCY NAME(S) AND ADDRESS(ES)	10. SPONSOR/MONITOR'S ACRONYM(S)
	11. SPONSOR/MONITOR'S REPORT NUMBER(S)

12. DISTRIBUTION/AVAILABILITY STATEMENT
Approved for public release; distribution unlimited

13. SUPPLEMENTARY NOTES
2013 AMOS (Advanced Maui Optical and Space Surveillance) Technical Conference, 10-13 Sep, Maui, HI.

14. ABSTRACT
We are developing a highly sensitive non-linear Curvature Wavefront Sensor (nlCWFS) which will make it possible to detect objects as dim as mv = 11 − 14. Current Space Situational Awareness (SSA) programs rely on laser guide stars (LGSs) to detect dim objects near GEOs, however LGSs are expensive to use and require permission to lase. The nlCWFS will be able to detect objects near GEOs without the use of a LGS and will be able to obtain higher contrast then possible with the SHWFS. The nlCWFS senses at the diffraction limit whereas currently used WFSs such as the SHWFS sense at the seeing limit. This difference awards the nlCWFS a gain in photon flux of (D r0)2 at low spatial modes such as tip-tilt. The SHWFS allows interference of points separated only by a subaperture making it insensitive to low order modes. The nlCWFS, on the other hand, uses the full spatial coherence of the pupil making it sensitive to low order modes which dominate the atmosphere and scatter light within a close angular separation of a GEO where a dim object might be hiding. In order to find dim objects near a bright target it is important to obtain a high contrast ratio within a small angular resolution of the central PSF core. The PSF contrast obtained with the nlCWFS is two orders of magnitude better than the SHWFS. In this paper we present results from building the nlCWFS for the 6.5 m MMT Smithsonian Observatory. We outline our progress towards building a nlCWFS for a 1.5 m telescope.

15. SUBJECT TERMS

16. SECURITY CLASSIFICATION OF:			17. LIMITATION OF ABSTRACT	18. NUMBER OF PAGES	19a. NAME OF RESPONSIBLE PERSON
a. REPORT **unclassified**	b. ABSTRACT **unclassified**	c. THIS PAGE **unclassified**	**Same as Report (SAR)**	**7**	

plane. At each propagation the phase is preserved and the the recorded intensity applied. The intensity is propagated between the pupil plane and the Fresnel plane till the phase converges.

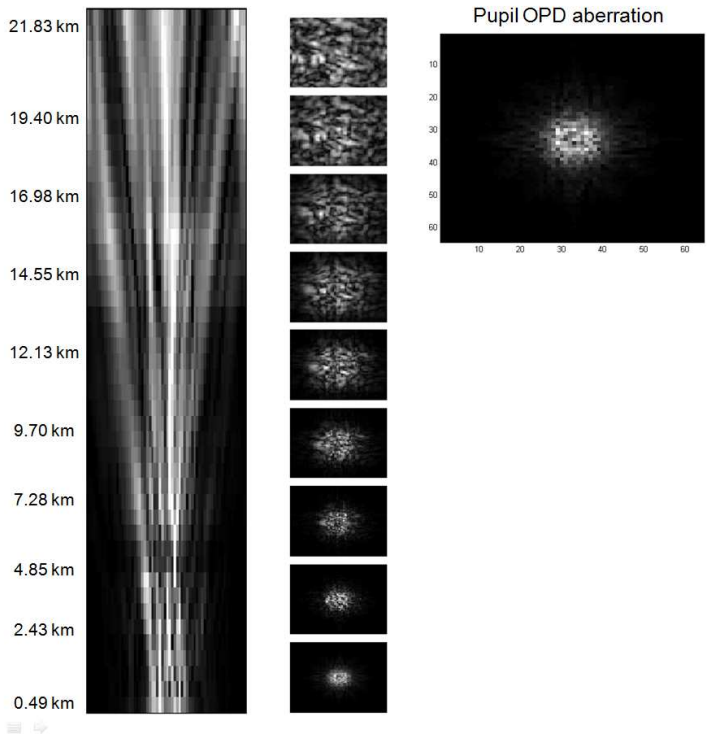

Fig. 1. As the image is propagated away from the pupil the rays become highly non-linear. The pupil optical path difference (OPD) aberration are shown in the top right. The propagation is for a 3.5 m telescope, $\lambda = 850$ nm, and, $r_0 = 0.068$ m. Several propagation distances are marked on the image.

We propose to build the nlCWFS which will use light from a bright object of visual magnitude $\mathrm{m}_v = 11-14$ to correct wavefront aberrated by atmospheric turbulence and detect dimmer objects, nearby. A Shack Hartmann Wavefront Sensor (SHWFS), when used with a 3.5 m telescope, can only detect a GEO of brightness $\mathrm{m}_v = 7$. The contrast achieved with the nlCWFS is two orders of magnitude better than that obtained with the SHWFS. As a result with the nlCWFS, a small sized dim object at a distance of $40,000$ km, near a GEO satellite, could be detected. Unlike current, conventional WFSs that sense at the seeing limit, the nlCWFS senses at the diffraction limit by extracting information form $\frac{\lambda}{D}$ speckles and by utilizing the full aperture of the telescope [9], where λ is the observation wavelength and D is the telescope diameter. With the use of the full aperture the nlCWFS can efficiently sense low-order aberrations which comprise the bulk of the wavefront error caused by atmospheric turbulence [5]. These low order aberrations scatter light within the central arc-second, where a dim object near a SSA asset might be hiding. Using wavefront spatial coherence over the entire aperture makes the sensor sensitive to low spatial frequencies. The increase in sensitivity, for low order modes, is equivalent to multiplying the source brightness by $(\frac{D}{r_0})^2$, here r_0 is Fried's parameter which gives the atmospheric coherence length. The size of a Shack-Hartmann (SH) subaperture is typically set equal to r_0. For the 1.5 m telescope the SHWFS requires 900 times more photons than the nlCWFS to reconstruct low order modes. The increased sensitivity of the nlCWFS allows detection of fainter objects and lower integration times when detecting brighter targets leading to an overall improvement in wavefront control.

2. SENSITIVITY COMPARISON BETWEEN THE nlCWFS AND THE SHWFS

The wavefront information which can theoretically be extracted from a given number of photons is defined as the "ideal" performance which can be reached by adaptive optics (AO) systems on ground-based telescopes [3]. For any single phase aberration mode (for example a Zernike mode in the pupil plane), the $1-\sigma$ measurement noise in a WFS is [9]:

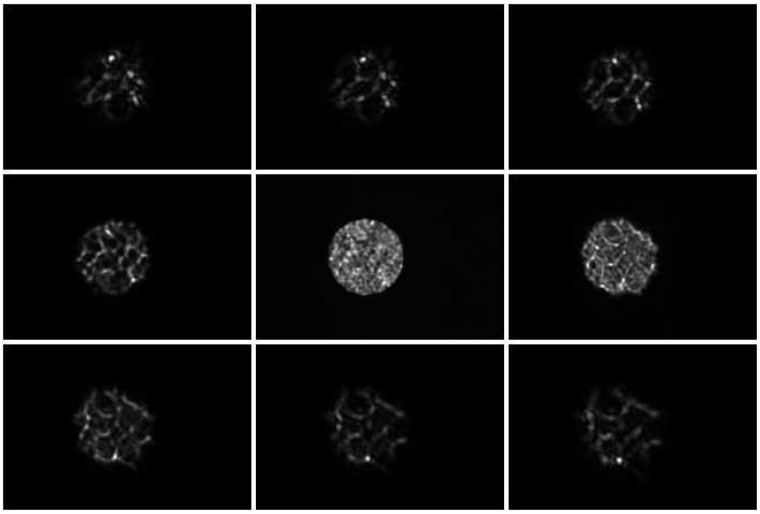

Fig. 2. Lab data showing images taken at several Fresnel propagation distance with the nlCWFS. You can see the speckle size go from large to small (frame 1 to 5, counting frames from top-left to bottom-right) as the detector moves towards the pupil plane and then get small to large (frame 6 to 9) as the detector moves away from the pupil plane. The spatial scale of the energy distribution among the speckles reflects the spatial scale of the frequencies to which you are most sensitive.

$$\Sigma = \frac{\beta}{2\sqrt{N_{ph}}} \tag{1}$$

where Σ is radians RMS in the pupil plane, N_{ph} is the total number of photons in the WFS, and β quantifies the WFS's sensitivity. Theoretically β is equal to 1. Σ is the standard deviation of the error for an unbiased estimator achieving the Cramer-Rao bound in the photon noise limit. For each WFS type there is a different β. A small β implies the Cramer-Rao bound is small as can be seen in Equation 1. For the nlCWFS $\beta = 1$ because the nlCWFS operates at the diffraction limit of the telescope. For the SHWFS, over the same spatial frequencies, β is higher by several orders of magnitude because it operates at the seeing limit. This can be understood by considering a low-order aberration like tip-tilt, the SHWFS measures the average lateral displacement of all the spot images. With increasingly small subapertures, the spot size grows but the total amount of light in the pupil remains the same, causing there to be less light in individual spots. This causes the measurement error to increase. The best way to measure tip-tilt would be by using a $\frac{\lambda}{D}$ wide spot. The nlCWFS does precisely this and measures tip-tilt as a displacement of a cloud of $\frac{\lambda}{D}$ speckles over the pupil. It is precisely this difference which leads to the $\frac{D}{r_0}$ improved sensitivity of the nlCWFS over the SHWFS. The SHWFS's poor sensitivity to low order aberrations is due to the large size of the PSFs produced by each subaperture and the nlCWFS's high sensitivity is due to the use of the full spatial coherence of the pupil by interfering light from opposite ends of the pupil.

When correcting 50 Zernike modes with a SHWFS with noiseless quad cells, $d_{sa} = r_0 = 0.05\,\text{m}$, over two cycles per aperture (cpa), β is equal to 21. For similar parameters $\beta = 1$ for the nlCWFS. Lab data was collected to calculate β for the nlCWFS and a theoretical β was calculated for the SHWFS using Equation 32 from Guyon's paper, Limits of Adaptive Optics for High Contrast Imaging [9] . The initial comparison shows that for an $8\,\text{m}$ telescope the SHWFS requires a 100 to 1000 times more photons than the nlCWFS, at low spatial frequencies, to reconstruct the wavefront [6]. We are interested in detecting dim objects within a small angular separation of a GEO; this requires obtaining a high PSF contrast within a small angular resolution of the core. The contrast to the central PSF peak for the SHWFS is 4.90×10^{-3} and for the nlCWFS is 3.02×10^{-5} for a $6.5\,\text{m}$ telescope, at observation wavelength of $650\,\text{nm}$, and $r_0 = 0.15\,\text{m}$ at $545\,\text{nm}$. For a $1.5\,\text{m}$ telescope, observation wavelength of $650\,\text{nm}$, and $r_0 = 0.05\,\text{m}$ at $545\,\text{nm}$ the SHWFS contrast is 4.58×10^{-2} and the nlCWFS contrast is 4.62×10^{-4}. The higher contrast obtained by the nlCWFS will enable us to find dim objects in close proximity to GEOs. The contrast calculation assumes that you are in the photon-noise limited range. This equation assumes perfect DM and detector and optimizes the speed at which the adaptive optics (AO) loop is running for each spatial frequency.

3. BUILDING THE nlCWFS FOR THE 6.5 M MMT

We built a nlCWFS for the 6.5 m MMT Smithsonian Observatory. The instrument is built on a 2 by 4 feet breadboard which gets mounted on the bottom of the telescope, see figure 3. The nlCWFS is designed to intercept light coming from the telescope before it reaches the SHWFS by using a 50-50 cube beam splitter. The beam splitter transmits half the light to the SHWFS and reflects the other half to mirrors nlCWFS-M1 and nlCWFS-M2. These two mirrors are remotely controlled to align the pupil and focal plane for the nlCWFS. Optics in front of the nlCWFS-M2, collimate, re-size, and re-image the pupil before light enters the Four Channel Assembly (FCA). The FCA consists of three dichroics that split the visual band into four channels creating the four Fresnel planes needed to reconstruct the wavefront. The Fresnel planes are created using the formula $dz = \frac{a^2}{\lambda N_f}$, where dz is the Fresnel propagation distance with respect to the pupil plane, a is the pupil radius, λ is the central wavelength of the band, and N_f is the Fresnel number. Each dichroic reflects light to a common imaging lens (nlCWFS-L4). By choosing a different object and image distance for each band we are able to create a different Fresnel propagation distance in color leading to the four Fresnel planes required to reconstruct the wavefront. The distance of each Fresnel plane with respect to the pupil and the central wavelength of the band used to create it is given in Table 1. In the lab we used a 1 mm pupil; the equivalent Fresnel plane distances for a 6.5 m telescope are also given. The Fresnel numbers match the original simulations carried out for an 8 m telescope [9].

Table 1. Creating Four Fresnel Planes

Fresnel Plane	Fresnel Number	Central Wavelength (nm)	Fresnel Propagation distance with respect to 1 mm pupil (mm)	Fresnel Propagation distance with respect to 6.5 m pupil (km)
1	5.38	865	53.72	3262.15
2	−5.38	642	−72.38	−2487.10
3	7.53	564	58.87	3058.08
4	−7.53	430	−77.21	−2269.70

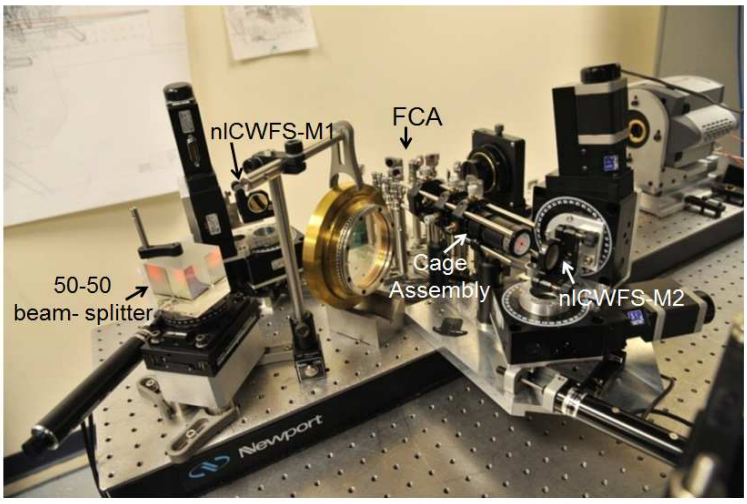

Fig. 3. nlCWFS built for the 6.5 m MMT AO Natural Guide-star system.

We carried out a successful mechanical fit for the nlCWFS on the MMT in April 2013. Optical alignment was performed manually. The four Fresnel plane images were created successfully and were similar to those obtained in the lab. During the fit we realized the diameter of the nlCWFS-M1 was too small and restricted alignment. The old nlCWFS-M1 mirror has been replaced with a larger diameter mirror and a fold mirror has been added to prevent the beam from being clipped by the cage-assembly, where the beam enters at a tight angle. We realized that the mounting brackets were not strong enough to support the instrument as the telescope moves therefore stable mounting brackets have been redesigned and fabricated. The updated system is currently in the process of being realigned and will be

ready for our upcoming observation run at the end of September 2013. We hope to obtain sky data with the nlCWFS, on the two awarded observing nights. The HR 8799 planet system [8] shown in figure 4 shows the current capability of the MMT AO system when used with a SHWFS. The MMT AO system was able to image planet d, which at a separation of 0.6 arc-seconds from the parent star has a Δm$= 9.2$ in L' band ($3.8\,\mu$m), at $0.9''$ seeing. With the nlCWFS we expect to extend the achievable contrast obtained by the MMT AO system by improving the WFS sensitivity. Simulations [9] show that at 1 cpa, for $\lambda = 850$ nm, and for D $= 8$ m the SHWFS (D/d = 16, here D is the pupil diameter and d is the size of the SH subaperture) requires approximately 150 times more photons than the nlCWFS to reach a given wavefront sensing accuracy.

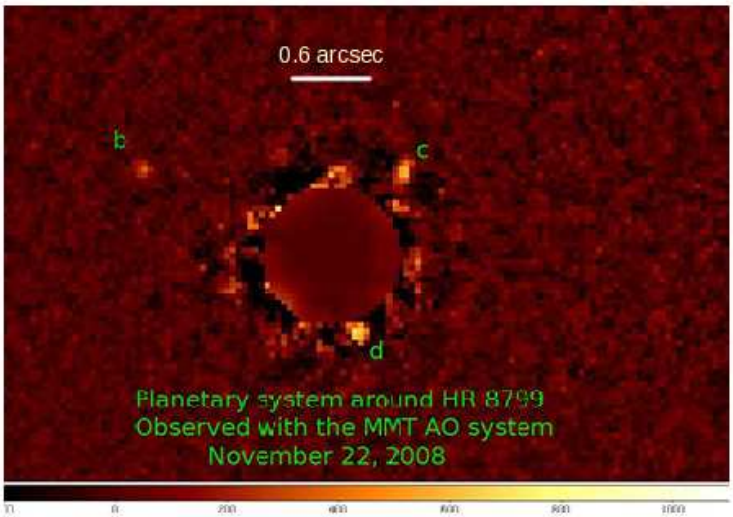

Fig. 4. Image at L' ($3.8\,\mu$m) of HR 8799 taken with the MMT AO system. All three components b, c, and d are detected at L'. Planet d is at a separation of $0.6''$ from the host star and has an apparent Vega magnitude of 14.39 ± 0.19 at L'. The seeing was $0.9''$ and the final image uses approximately 90 minutes of data [8].

4. DEFORMABLE MIRROR GENERATED 4 PLANES

The Deformable Mirror Generated 4 Plane (DMG4P) experiment used bench-source data from an operational 3.5 m telescope equipped with adaptive optics. There are two reasons for doing this, first, to match simulations with telescope data and second, to test the nlCWFS reconstructor with actual telescope data. In the DMG4P experiment we generate the four Fresnel planes needed for nlCWFS reconstruction by putting focus on the deformable mirror (DM). We start by using an unaberrated spot to which four different amounts of focus is added by moving the DM. The generation of the four defocused spots is equivalent to obtaining the image in four different Fresnel planes. The Fresnel plane distances used are $\mathrm{dz}_1 = 5.21 \times 10^5$ m and $\mathrm{dz}_2 = 7.30 \times 10^5$ m out of pupil; two planes generated on either side of the pupil plane. The Fresnel numbers match the original simulations done Guyon [9]. In order to simplify our experiment we us Zernike modes to create the optical path difference (OPD) aberration in the pupil plane instead of using the atmospheric turbulence generator to create atmospheric turbulence. The different Zernikes used in the experiment are focus, astigmatism, and coma. Each of these aberrated images are propagated by dz_1 and dz_2 on either side of the pupil plane. The four out-of-pupil or Fresnel plane images for one radian of astigmatism in the pupil plane are shown in figure 5. The top row shows actual data obtained with the telescope and the bottom row shows simulated data. We are in the process of reconstructing these images with the nlCWFS reconstructor. We have been able to successfully reconstruct lab data demonstrating that the nlCWFS reconstruction algorithm works [5].

5. CONCLUSION AND FUTURE WORK

In this paper we make the case that the nlCWFS is a more sensitive sensor than the SHWFS. The ability of the nlCWFS to utilize the spatial coherence of the entire pupil, compared to the SHWFS which splits the pupil into subapertures, makes it more sensitive to low order aberrations which dominate the atmosphere and scatter light on to a dim object

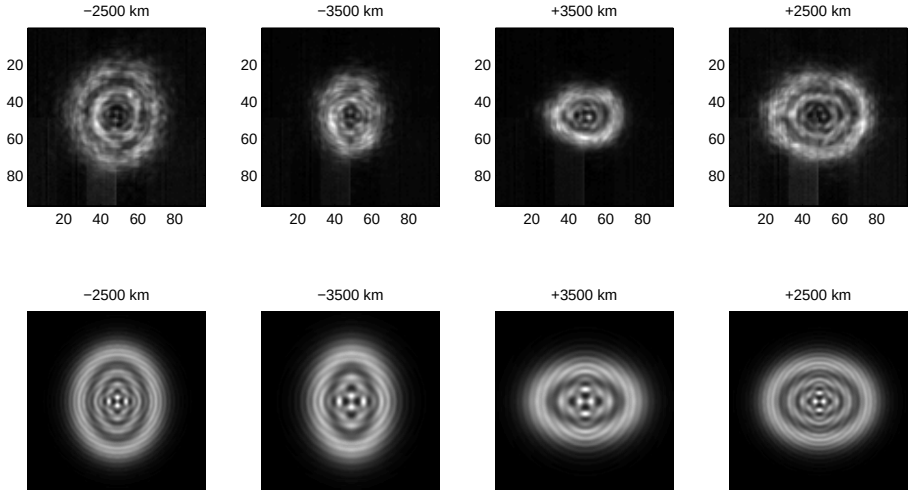

Fig. 5. The top row shows the four Fresnel planes obtained with the 3.5 m telescope in the DMG4P test. The bottom row shows the simulated planes.

that may be hiding close to a GEO. We show that the nlCWFS can achieve contrasts greater than those obtainable with the SHWFS; making the nlCWFS an ideal WFS for searching for dim objects near bright GEOs. The nlCWFS is sensitive enough to be used with out a laser guide-star which significantly lowers the cost of AO operations and eliminates the need to obtain permission. Through the DMG4P test we demonstrate that, our wave-optics model is able to accurately simulate the Fresnel planes need for the nlCWFS reconstruction and that the model can be used to carry out the detailed optical sensitivity analysis. We provide a status summary of a nlCWFS build for the 6.5 m MMT AO system and show the increase in contrast that can be obtained. We are scheduled to make our first observations with the nlCWFS over the next few months.

We have developed wave-optics simulations for a 1.5 m and a 3.5 m telescope in which we close the loop with the SHWFS for various turbulence parameters; we are in the process of refining the nlCWFS reconstructor and incorporating it in a closed loop simulation so that we can compare the quality of wavefront reconstruction with both sensors. We want to quantify the amount of photons needed per spatial frequency by each WFS to be able to reconstruct the wavefront with a given signal-to-noise ratio. Theory predicts that the nlCWFS requires fewer photons compared the the SHWFS, we would like to demonstrate this with simulated, lab, and sky data. To complete this task we plan on building the nlCWFS for an existing 1.5 m telescope equipped with AO.

6. ACKNOWLEDGMENTS

The authors wish to thank Michael Oliker for coming up with the DMG4P test and for collecting data for the experiment.

References

1. F. Roddier, M. Northcott, and J. E. Graves. A simple low-order adaptive optics system for near-infrared applications. *PASP*, 103:131–149, January 1991.
2. O. Guyon. Ultra-high-sensitivity wavefront sensing for extreme-AO. In *Society of Photo-Optical Instrumentation Engineers (SPIE) Conference Series*, volume 7015 of *Presented at the Society of Photo-Optical Instrumentation Engineers (SPIE) Conference*, July 2008.
3. O. Guyon. Limits of Adaptive Optics for High-Contrast Imaging. *Astrophys. J.* , 629:592–614, August 2005.
4. O. Guyon, C. Blain, H. Takami, Y. Hayano, M. Hattori, and M. Watanabe. Improving the Sensitivity of Astronomical Curvature Wavefront Sensor Using Dual-Stroke Curvature. *PASP*, 120:655–664, May 2008.
5. M. Mateen, V. Garrel, M. Hart, and O. Guyon. Results from the laboratory demonstration of the nonlinear curvature wavefront sensor. In *Society of Photo-Optical Instrumentation Engineers (SPIE) Conference Series*, volume 7736 of *Society of Photo-Optical Instrumentation Engineers (SPIE) Conference Series*, July 2010.

6. M. Mateen, O. Guyon, J. Sasian, M. Hart, and V. Garrel. non-linear Curvature Wavefront Sensor for Extremely Large Telescopes. *Second International Conference On Adaptive Optics Extremely Large Telescopes*, 2, September 2011.
7. R. W. Gerchberg and W. O. Saxton. A practical algorithm for determination of the phase from image and diffraction planes. *Optik*, 35:237–246, December 1972.
8. P. M. Hinz, T. J. Rodigas, M. A. Kenworthy, S. Sivanandam, A. N. Heinze, E. E. Mamajek, and M. R. Meyer. Thermal Infrared MMTAO Observations of the HR 8799 Planetary System. *Astrophys. J.* , 716:417–426, June 2010.
9. O. Guyon. High Sensitivity Wavefront Sensing with a Nonlinear Curvature Wavefront Sensor. *PASP*, 122:49–62, January 2010.